Application of Analytic Morphomics for Belted Elderly Occupants in Frontal Crashes

Susumu Ejima, Sven A. Holcombe, Peng Zhang, Brian A. Derstine, Rebecca L. Goulson,
Joel M. Williams, Carla Kohoyda-Inglis, Stewart C. Wang

Abstract In this study, we used analytic morphomics to understand the mechanisms of rib fracture for older occupants in frontal crashes. Analytic morphomics extracts body features from computed tomography scans of people involved in vehicle crashes who have been treated at the University of Michigan, a Level-1 trauma center. Chest injury and rib fracture patterns were examined in belted, front row occupants involved in frontal crashes from the International Center for Automotive Medicine database. Among these occupants, two age groups (younger and older) with the maximum abbreviated injury scale of chest region $\geq$ 3 ($MAIS_{thx}$ 3+) were categorized. The location of each rib fracture was compared between the groups. Regression analyses were conducted to investigate fracture outcomes considering risk factors including vehicle, demographics, and morphomics. The rib fractures of belted occupants were mainly located under the path of the shoulder belt. For the older group, fracture patterns tended to be located in the anterior region but also bilaterally. Moreover, morphomic factors related to rib shape are the major driver of rib fracture for the older group. The current results for rib shape can highlight the importance of considering these morphomics characteristics when assessing chest injury and creating elderly computer models.

Keywords analytic morphomics, automotive medicine, elderly, frontal crashes, rib fracture,

I. INTRODUCTION

According to the "World Population Prospects" from the United Nation's report [1], Japan is the most aged country in the world. This situation is predicted to worsen in Japan and to expand into developed motorized countries such as European countries, Korea, and China. In 2015, the number of fatalities resulting from road traffic crashes in Japan was 4,117, which is an increase of 0.1 percent from 4,113 in 2014 [2]. This is the first increase in 15 years, and includes a large increase in fatalities among the elderly. Road safety that responds to the demographic shift and the wide diversity of motor vehicle crashes in the real world is imperative.

In the discussion of automobile crash safety, it must be considered that occupant factors such as age, gender, and body habitus contribute to injury outcome. Thus, it is essential to examine injury mechanisms from a medical perspective. Moreover, when we consider traffic safety, it is important to understand the relationship between the crash and the individual characteristics of the injured occupant. However, humans have a large number of biological tissues inter-related in complex ways, and we still lack a quantitative understanding of the relation between the magnitude of an impact and the resulting damage.

The thorax is a major injury location in motor vehicle crash occupants. Thoracic trauma is the principal cause of 30% of road traffic deaths [3]. The thorax houses a variety of critical physiological processes. The chest region contains the primary elements of the respiratory and circulatory systems, and the rib cage protects the inner organs, including the liver, spleen, kidneys, and stomach. It is evident that the chest, more than any other body region, is particularly vulnerable to crash injury as the subject ages. The total injury rates are higher in elderly motor vehicle crash occupants than in younger occupants and there are significant differences in their respective injury patterns, particularly thoracic, in incidence and severity.

Geometric properties of the ribcage, such as rib angle, have also been linked to rib fracture risk [4]. Current anthropomorphic test dummies (ATDs) lack the biofidelity required in the ribcage area to predict specific injuries, while difficulties in cadaver test setup and repeatability limit such tests as predictive tools. Therefore, computational methods such as finite element human body modelling are seen as offering significant benefits

S. Ejima is a Research Associate Professor of the International Center for Automotive Medicine at the University of Michigan, USA (+1-734-763-1807 and sejima@umich.edu). SA. Holcombe is a Crash Research Engineer, P. Zhang is a Research Assistant Professor, BA. Derstine is a Data Scientist, RL. Goulson is a Research Assistant, JM. Williams is Crash Investigator, C. Kohoyda-Inglis is a Program Director and SC. Wang is Endowed Professor from the International Center for Automotive Medicine at the University of Michigan.

to the study of the ribcage and the relationship between vehicle collisions and high energy traumatic injuries. While recent finite element human models represent elderly [5-6], obese [7], and female [8-9] occupants, these models do not specifically represent the individuals in motor vehicle crashes (MVCs) exposed to loading and injury. In statistical analyses of field crash data where a hypothesis is that the individuality of each occupant contributes to their injury outcome, the use of just one model would make it difficult to actually represent that individuality via finite element models. For this reason, the personalized finite element models [10] via geometrical morphing would be useful in this kind of injury prediction. One role that morphomic can contribute is to help identify some of key features to modify when making personalized or scalable/morphable finite element models and this would benefit groups who are deciding on how best to implement a ribcage scaling/morphing tool.

Studies [11-12] proposed a novel method to characterize human rib geometry directly from CT scans of the chest using a limited set of quantifiable parameters. The method, *analytic morphomics*, includes techniques for the processing of CT data to collect measures of overall ribcage anatomy and bone density information in a consistent manner. By using this information, we could obtain not only the geometric variation within the population, but also the relationship between the crash and characteristics of the injured occupant by examining real-world crash cases.

In this study, we used analytic morphomics to understand the mechanisms of rib fracture for elderly occupants in frontal crashes. Analytic morphomics extracts body geometry and composition data from CT scans of people involved in vehicle crashes who have been treated at the University of Michigan in the US, a Level-1 trauma center. Based on these images, the features of rib shape, such as rib dimensions, curvatures, and the rib inner angles were measured. By using this data set, which includes crash and medical data, the characterization of rib fractures in elderly occupants is quantified. This systematic methodology allows our analysis to accurately represent injury outcomes in frontal crashes and provides the robustness for targeting a specific injury from real-world crash cases. By using this methodology, it becomes possible to build a flexible human model to quantify the effect of human characteristics for thoracic injury.

II. METHODS

ICAM database

The crash data were obtained from the University of Michigan International Center for Automotive Medicine (ICAM) database for calendar years 1996-2015. ICAM was one of the founding centers of the Crash Injury Research and Engineering Network (CIREN) that collects and analyses the most detailed crash injury data. Since 2011, ICAM has expanded not only its severity criteria but also the crash types, such as pedestrian and bicyclist, who have been treated at the University of Michigan. In-depth investigations of the case occupant's vehicle and crash scene, with police reports, are conducted based on standard National Automotive Sampling System (NASS) protocol. Detailed crash case study is performed to estimate the injury pattern and the kinematics of the person involved in the accident. The accident data are linked to medical records of the case occupant's injuries. These records include emergency medical care by paramedics, radiological images, operative notes, clinical progress, treatment, interviews, and discharge reports. The multidisciplinary review and discussion of each case is conducted by an experienced ICAM accident investigator, a biomechanical engineer with experience in impact biomechanics research, a trauma physician, and dozens of automotive safety engineers to derive the causation of the injuries based on the physical evidence, medical knowledge, and injury biomechanics from the engineering point of view. In addition, analytic morphmics is utilized to quantify the occupant characteristics based on the medical imaging data to understand more about the injury mechanisms. These reviews reconfirm the crash severity and injury assessment in the real-world crash.

Inclusion criteria for the current study were based on the following vehicle and crash parameters: vehicle model year was 1990 or newer, the principal direction of force (PDOF) was between -45 degree and 45 degree, and, in the cases with multiple impacts only the primary impact was considered. Vehicles that sustained a non-horizontal event such as a rollover were excluded. The occupant and injury parameters were based on the following criteria: occupant was older than 15 years and seated with 3-point belt in the right or left front outboard seating position, an Abbreviated Injury Scale (AIS) of each body region was available, and an available thoracic CT scan. The total number of case occupants fitting these inclusion criteria was 228. Occupants were categorized by age in either the under 60 (younger) group or 60 and over (older) group based on the literature[13] which indicates the average age threshold was 61 years for AIS 3 fractures. Table I shows the vehicle, injury and demographic data used in current analysis. In this study, the Maximum Abbreviated Injury Scale (MAIS) was assessed separately for each occupant with thoracic injuries (MAISthx).

TABLE I
VEHICLE, INJURY AND DEMOGRAPHIC DATA

Vehicle		
Crash severity	mph	Change in vehicle velocity (delta V) or equivalent barrier speed (EBS).
Intrusion count	-	The total number of result displacement of intrusions to all vehicle compartments.
Longitudinal intrusion	cm	The sum of longitudinal intrusion in the lower, mid-, and upper instrumental panel area and as the number of intruded area.
Injury		
MAISthx	-	Maximum Abbreviated Injury Scale (MAIS) of chest region.
Demographics		
Age	years	Younger goup: Age under 60, Older group: Age 60 and over
Height	cm	The standard height of the occupants.
Weight	kg	The standard weight of the occupants.
Body Mass Index (BMI)	$kg/(m^2)$	Calculated by dividing the patient's mass by the square of his or her height.
Gender	-	Male / Female

Fracture delineation

In the ICAM data collection system, medical records were examined to find the number of rib fractures and side of fractures (left or right) previously identified by a board-certified radiologist and coded by the ICAM team. In the meantime, the precise 3-dimensional location of rib fractures present in CT scans from the ICAM population of car crash occupants was documented. This protocol was used to develop a database associating fractures in their spatial locations with rib framework curves defined for each rib using a semi-automatic image processing system. Using this method, the location is recoded as a point in the scan coordinate system, shown in Fig. 1, as well as a location (percentage length from the proximal end of rib and polar angle relative to an origin half-way between the spine and the sternum) along the rib, shown in Fig. 2. For the current study, polar angle of each fracture point was utilized for quantifying locations of rib fractures. With this polar angle, the fracture locations were categorized into five segments (A: Anterior, AL: Antero-Lateral, L: Lateral, PL: Postero-Lateral, and P: Posterior) [14]. Each segment has 36 degrees in the mid-sagittal plane. The location of rib fracture for the passenger side was mirrored to the opposite side, in order to combine driver and passenger data.

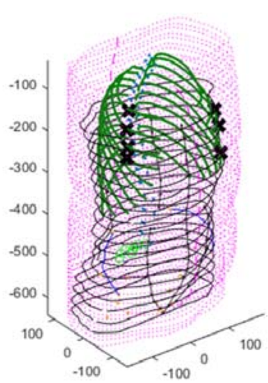

Fig. 1. 3-dimensional location of rib fractures with ribcage coordinate system

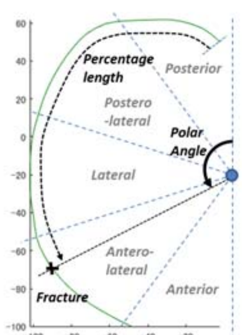

Fig. 2. Percentage length and polar angle to identify the rib fracture location in five area by using published method [14]

Analytic morphomics data

The University of Michigan Review Board approved the use of the standard CT scans available for each occupant for this study (HUM00043599 and HUM00041441). CTs were obtained from the University of Michigan radiology registry. Each occupant was subjected to quantitative CT scanner architectures with automatic exposure control. The scans were processed semi-automatically using custom algorithm written in MATLAB 2015a (The Mathworks Inc., Natick, MA, USA). All subjects were lying flat on the scanning table during each scan. The slice thickness of all scans ranged from 0.625 to 5 mm and spatial resolution within each slice from 0.3 to 1.1mm. The following rib morphomic variables were assessed based on the need to represent the in-plane shape of the ribs defined by [12]. Measurement items are illustrated in Table II. Measuring a fractured rib could confound the normal, appropriate, value. To avoid this variation, the following protocol is applied for a given rib of an occupant: if neither side is fractured, return the average left/right measure; if one side is fractured, return the other side measure only; if both sides are fractured, this rib is excluded.

TABLE II
RIB MORPHOMICS MEASUREMENTS OBTAINED FROM CT SCANS

Variables	Units	Description	
Rib Size (S_x)	mm	Linear distance between rib ends	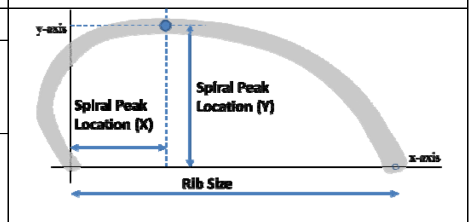
Spiral Peak Location (X)	mm/S_x	Location of spiral peak along the X-axis, normalised by rib end-to-end length (**Rib Size**)	
Spiral Peak Location (Y)	mm/S_x	Location of spiral peak along the Y-axis, normalised by rib end-to-end length (**Rib Size**)	
Dist. end curvature	mm/S_x	Curvature at the distal end of the rib (higher number means smaller radius of curvature)	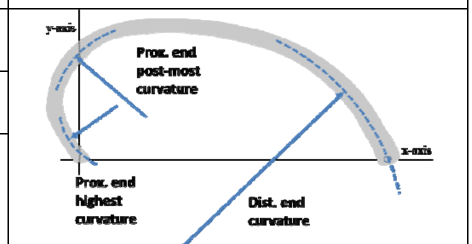
Prox. end highest curvature	mm/S_x	Curvature at the proximal end of the rib (location of max curvature)	
Prox. end post-most curvature	mm/S_x	Curvature at the proximal end of the rib (location of posterior-most extension)	
Dist. end inner angle	deg.	Inner angle of the end of the rib and the x-axis	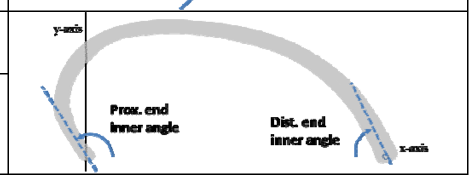
Prox. end inner angle	deg.	Inner angle of the start of the rib and the x-axis	

Statistical Analysis for rib fracture

Utilizing the serious injury data ($MAIS_{thx}$ 3+) and rib fracture pattern due to frontal crashes in the ICAM database, univariate and multivariate regression analyses were conducted to investigate the association between rib shape and rib fracture. Rib number five, selected in this study, shows a high rib fracture incidence ratio for the older group. The concept of using statistical approach is to predict the rib fracture risk and the importance of each variable defined with a predictive model [15-16].

Logistic regression models were fitted to investigate rib fracture risk with different configurations of crash, demographic, and morphomics variables for occupants without and with rib fracture. The statistical analysis was based on the combination of the ICAM crash database (vehicle and demographics) and the morphomics database. There are 228 cases available with occupants involved in frontal crashes, among which there are 102 cases with complete processed rib five morphomic data without both sides fractured. Rib fractures for occupants involved in frontal crashes were identified by the morphomics database. The data was separated into two groups: with fracture and without fracture at the rib five. The data analysis was conducted using MATLAB2015a statistical tool box.

The selection of each variable is based on the knowledge of characterization of ribs [11],[17] and the evaluation with Akaike information criteria (AIC). AIC is an information criteria that addresses the trade-off between the goodness of fit of the model and the complexity of the model. The performance of regression models was assessed with AIC and receiver operating characteristic (ROC) which plots the model sensitivity as a function of specificity. The performance of the models was compared using area under the curve (AUC).

There were 10 covariate variables examined: two vehicle (*Crash severity, Intrusion Count*), three demographic (*Age, BMI, Gender*), and five morphomic (*Spiral Peak Location, Prox. end highest curvature, Prox. end posterior most curvature, Dist. end inner angle, Prox. end inner angle*). The models were characterized into four different scenarios to assess the individual variable contribution on rib fracture risk. Scenario 1 used vehicle variables; Scenario 2 vehicle and demographic variables; Scenario 3 vehicle and morphomics variables; and Scenario 4 used all variables. We then used AIC and AUC to determine the performance of developed predictive models under different scenarios.

III. RESULTS

There were 228 belted occupants who met the inclusion criteria of this study. By using vehicle and demographic data, elderly features were compared with the younger group who sustained $MAIS_{thx}$ 3+ injuries. Among 228 occupants, there were 47 younger occupants with $MAIS_{thx}$ 3+ and 42 older occupants with $MAIS_{thx}$ 3+. Average age for the younger and older group is 42 and 72 years respectively. Table III shows the result of the univariate analysis for the vehicle and demographic variables. The table includes mean, standard errors, and *P* values obtained from two-sample *t* tests for continuous variables. It also provides the counts and the percentage for categorical variables (*Gender*) of each group, the *P* value from the Fisher's exact tests. While the older group had a lower severity and less intrusion compare to the younger group, there are no significant differences in the demographic variables in both groups except age.

Out of the younger group (n=47) and older group (n=42) who sustained $MAIS_{thx}$ 3+ injuries, we were able to obtain complete 3-dimensional locations of all rib fractures from 28 younger occupants and 37 older occupants. Figure 3 shows the distribution of where these fractures occurred with respect to subject rib number between the younger and older groups. X-axis shows the rib number and Y-axis show the rib fracture incidence rate determined by dividing the number of fractured ribs at each rib by the number of age group with rib fracture. Older occupants had significantly more fractured ribs than younger group at ribs 4, 5, and 6 where the shoulder belt was most likely to be contacting the body.

Figure 4 shows exact rib fracture location along the rib categorized into five segments (A: Anterior, AL: Antero-Lateral, L: Lateral, PL: Postero-Lateral, and P: Posterior). Figure 4(a) is the younger group and Figure 4(b) is the older group. X-axis shows polar angle and from 0 to -180 degree indicates inboard (driver's right side) and 0 to 180 degree indicates the outboard (driver's left side). Y-axis shows the rib number. The rib fractures of belted occupants were mainly located under the path of the shoulder belt and locations of rib fracture are concentrated inboard in both age groups. For the elderly group, fracture patterns tended to be located in the anterior-lateral region but also bilaterally compared to the younger group.

TABLE III
SUMMARY OF STATISTICAL FOR $MAIS_{THX}$ 3+ OCCUPANTS BY AGE GROUP

Variables	MAISthx 3+ Age under 60 (n=47) Mean or count	Age under 60 (n=47) Std error or percent	Age 60 and over (n=42) Mean or count	Age 60 and over (n=42) Std error or percent	p-Value	
Vehicle						
Severity	36.128	12.465	27.643	9.723	0.001	**
Intrusion count	3.213	1.910	1.381	1.413	0.000	**
Long. Intrusion	48.319	37.615	14.714	28.733	0.000	**
Demographics						
Age	42.000	12.585	72.000	8.027	0.000	**
Height	171.000	9.084	169.357	10.250	0.428	
Weight	91.404	33.146	81.810	22.415	0.110	
BMI	31.110	10.513	28.198	6.038	0.109	
Male	22	46.8%	16	38.1%	0.852	

** p<0.01

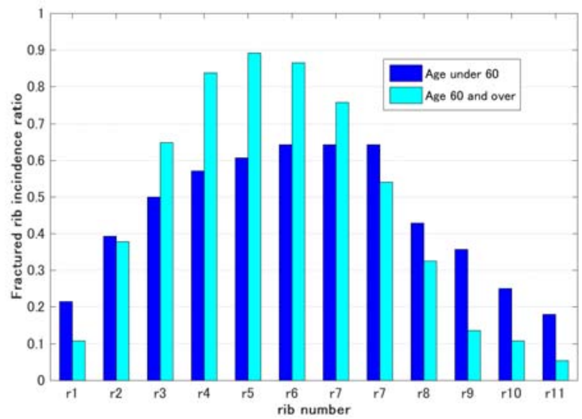

Fig. 3. Fractured rib incidence ratio between younger and older group

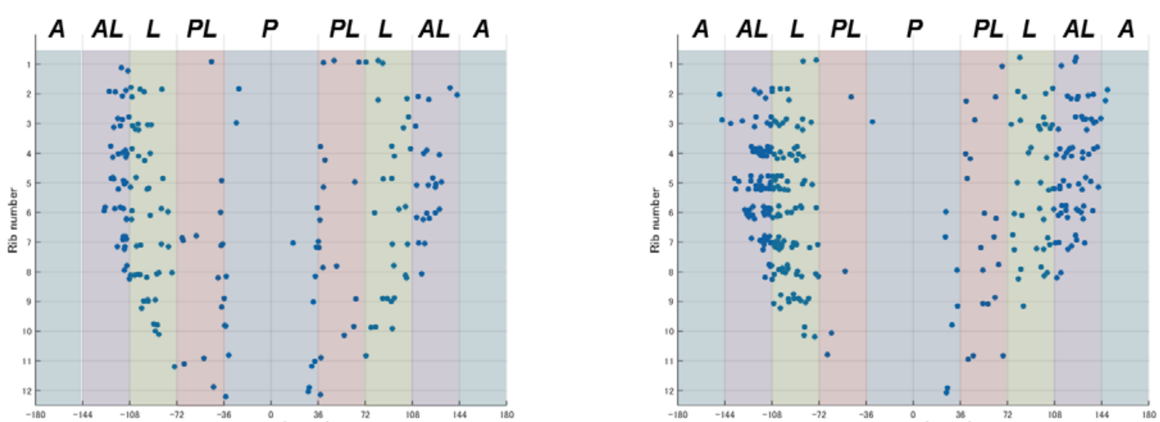

(a) Age under 60 (n=28) (b) Age 60 and over (n=37).

Fig. 4. Rib fracture location at each rib number

According to the rib fracture incidence ratio and location using $MAIS_{thx}$ 3+ criteria, the older group had significantly more fractures at ribs 4, 5, and 6 and the fracture locations along the rib shifted more toward the anterior region. From this result, rib 5, which indicates the highest rib fracture risk in the older group was chosen as a predictor for analyzing with vehicle, demographic, and morphomics variables. For the 102 occupants with available rib morphomics variables, a logistic regression model was applied to quantify the contribution of rib shape by linking the morphomic database with the ICAM database. Table IV presents a univariate analysis of the selected 10 variables. Table IV includes mean, standard errors, *t* statistics, and *P* values obtained from two-sample *t* tests for continuous variables. It also provides the counts and the percentage for categorical variables (*Gender*) of each group, the *P* value from the Fisher's exact tests. Various features were compared between the groups of occupants without rib 5 fractures and with rib 5 fractures. Among the vehicle variables, *Intrusion count* was the most significant. *Age* was the most significant variable overall. The result suggests that an increase in age is significantly associated with risk of rib fracture. Among the various morphomics variables, *Prox. end highest curvature* and *Prox. end inner angle* were significantly different between the two groups with *P* value 0.002.

TABLE IV
SUMMARY OF STATISTIC BETWEEN THE GROUPS OF OCCUPANTS WITHOUT RIB 5 FRACTURES AND WITH RIB 5 FRACTURES

Variables	Without rib fracure (n=68)		With Rib fracture (n= 34)		p-Value	
	Mean or count	Std error or percent	Mean or count	Std error or percent		
Vehicle						
Severity	30.456	12.145	28.059	10.759	0.313	
Intrusion count	2.794	1.989	1.971	1.883	0.045	*
Demographics						
Age	46.132	19.308	62.029	18.599	0.000	**
BMI	30.423	8.630	30.023	7.980	0.817	
Male	30	44.1%	18	52.9%	0.264	
Morphomics						
Spiral Peak Location (X)	0.318	0.040	0.309	0.037	0.276	
Prox end highest curvature	5.713	1.369	6.669	1.428	0.002	**
Prox end post-most curvature	3.401	0.374	3.511	0.343	0.142	
Dist end inner angle	79.557	7.131	77.620	10.046	0.320	
Prox end inner angle	111.231	6.498	117.971	11.361	0.002	**

* p<0.05 ** p<0.01

The logistic regression models were fitted with different configurations of variables predictive of rib fracture and were evaluated by the AIC in the multivariate analysis of the 10 variables selected. Figure 5 shows the progression of ROC curves from the statistical model of rib fracture rate using vehicle, demographic, and morphomic data. The model developed based solely on vehicle data had an AUC of 0.63. The model prediction improved when combining vehicle and demographic data with an AUC of 0.74. The AUC associated with vehicle and morphomics data was 0.78 and increased to 0.86 when combining vehicle, demographic, and morphomics variables.

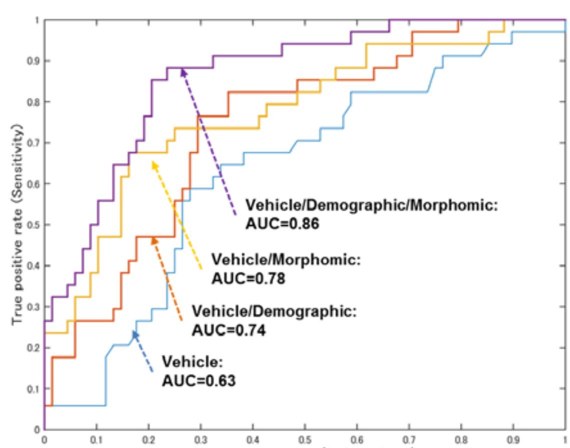

Fig. 5 Progression of receiver operating characteristic curves of different scenarios

Table V shows the coefficient, error, and *P* values in predicting rib fracture from regression analysis in each scenario. The most important morphomics variable was *Prox. end inner angle*. *Age* was most important when combined with the vehicle and demographic variables. However, when morphomics were combined with both demographic and vehicle variables, *Age* became less important. The age decrease in importance can be explained by collinearity between age and morphomic variable such as *Prox. end highest curvature* and *Prox. end inner angle*.

Figures 6 and 7 show the scatter plot of without and with rib 5 fracture occupants of *Prox. end highest curvature and Prox. end inner angle* with respect to the age. Triangles indicate 34 occupants with rib 5 fracture and circles indicate 68 occupants without rib 5 fracture. The occupants with rib 5 fracture are distributed in large *Prox. end highest curvature* and *Prox. end inner angle* and it also increases with age.

TABLE V

ESTIMATION OF COEFFICIENTS FOR VARIABLES DIFFERENT SCENARIO

Variables	Estimate	SE	p-Value	
Scenario 1				
Vehicle				
(Intercept)	0.034	0.584	0.954	
Severity	-0.008	0.019	0.689	
Intrusion count	-0.211	0.120	0.080	
Scenario 2				
Vehicle				
(Intercept)	-3.417	1.669	0.041	
Severity	0.013	0.022	0.557	
Intrusion count	-0.088	0.137	0.521	
Demographics				
Age	0.043	0.015	0.003	*
BMI	0.000	0.029	0.999	
Gender	0.465	0.472	0.325	
Scenario 3				
Vehicle				
(Intercept)	-82.428	31.783	0.010	
Severity	0.004	0.025	0.870	
Intrusion count	-0.228	0.140	0.103	
Morphomics				
Spiral Peak Location (X)	76.660	33.091	0.021	*
Prox end highest curvature	-1.132	0.611	0.064	
Prox end post-most curvature	9.742	4.129	0.018	*
Dist end inner angle	-0.008	0.036	0.824	
Prox end inner angle	0.281	0.096	0.003	**
Scenario 4				
Vehicle				
(Intercept)	-128.535	39.026	0.001	
Severity	0.017	0.028	0.545	
Intrusion count	-0.272	0.171	0.111	
Demographics				
age	0.041	0.018	0.024	*
bmi	0.015	0.037	0.678	
gender	1.702	0.656	0.009	**
Morphomics				
Spiral Peak Location (X)	119.385	39.566	0.003	**
Prox end highest curvature	-2.038	0.755	0.007	**
Prox end post-most curvature	14.698	4.898	0.003	**
Dist end inner angle	0.012	0.040	0.773	
Prox end inner angle	0.419	0.120	0.000	**

* p<0.05 **p<0.01

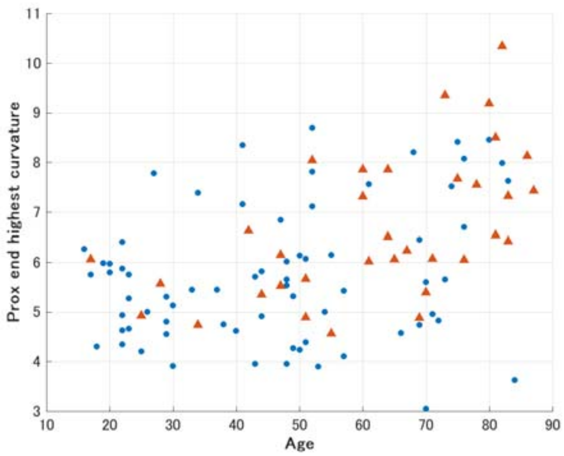

Fig. 6 Fractured Rib 5 prox. end highest curvature with respect to the age

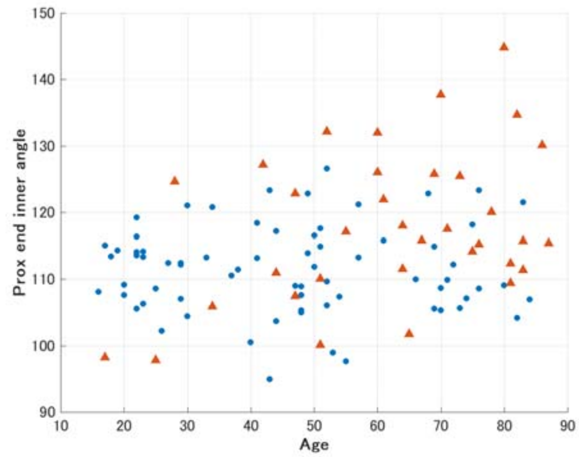

Fig. 7 Fractured Rib 5 prox. end inner angle with respect to the age

IV. DISCUSSION

The ICAM crash data collection system is based on the identification and documentation of injury causation, and this system can define all the factors that are believed to be necessary for the occurrence and/or severity of injury. The advantage of crash data collection in a trauma center is to integrate data that includes medical imaging such as CT, X-ray, and MRI, which indicate the location of the fracture or the tissue damage constituting the injury. In addition, the image data provide effective information for predicting injury patterns related to the particular type of loading or mechanical response that can estimate not only the strength of the bone but also the geometry change with age. In this study the elderly variables involved in frontal crashes and causation of rib fracture are summarized by using real-world crash cases.

According to the univariate analysis with $MAIS_{thx}$ 3+ and rib fracture incidence ratio, older occupants sustained more fractured ribs at lower crash severity and with less intrusion compared to the younger occupants. This result indicates that the seat belt is the main involved physical component (IPC) of $MAIS_{thx}$ 3+ older occupants. This phenomenon is consistent with prior studies [18-19] which show the common IPC of elderly (older than 75) occupants is the seat belt.

The ICAM database captures the location of rib fractures with much more detail and precision than previously available. Utilizing this system to analyze the rib cages of ICAM study subjects who have sustained chest wall injures shows clear variation in the pattern of rib fracture observed in younger versus older occupants. Older occupants' rib fractures tend to occur more anteriorly while younger occupants' fractures occur more laterally. This result shows a similar trend along with rib fracture patterns in various restraint statuses, when compared to the CIREN database [19]. The age related changes increase the risk of rib fracture due to the geometry or material changes along the ribs [20]. According to the study of analytic morphomics with ribs [11], rib shape change has a potential to affect fracture location and loading path from seatbelt in frontal crashes. For this reason, the logistic regression analysis is applied to clarify the effect of rib shape by using morphomics variables linked to the crash case.

The results obtained in this study highlight the importance of morphomics variables in predicting rib fracture risk. The effect of two vehicle, three demographic, and five morphomics variables on the risk of rib fracture in frontal crashes are assessed by using ROC curve. The results indicated that the effect of morphomics variables improved the prediction of occupant rib fracture risk. The AUC, obtained in Scenario 4 where morphomics data was added to the vehicle and demographic data, was greater than the AUC obtained when using vehicle and morphomics data (Scenario 3), significantly greater than when using vehicle and demographic data (Scenario 2), and when using vehicle data alone (Scenario 1).

Prox. end inner angle, *Prox. end highest curvature*, *Prox. end post most curvature*, and *Spiral peak location* were among the most significant morphomics variables of rib fracture in frontal impact in the multivariate models. In addition, *Prox. end inner angle* and *Prox. end highest curvature* were significant in the univariate analysis as shown in Table IV. This indicates that these two factors are good surrogates for rib fracture risk and provide rib shape information in the prediction model. Figure 8 indicates the sagittal image at the start point of rib 5 for younger and older occupants. The rib shape of younger occupants who have small *Prox. end inner angle* and *Prox. end highest curvature* shows a round shape and the rib shape of older occupants who have a large *Prox. end inner angle* and *Prox. end highest curvature* shows a vertically long elliptic shape. *Prox. end inner angle* is the exit angle at the proximal end of the rib and *Prox. end highest curvature* is related to the curvature of the rib shape. These factors could change the boundary conditions with respect to frontal load with a belt as well as change the rib fracture location. These results suggest the rib shape is also important as well as material properties when we discuss rib fracture. The next step of this study with finite element models clarifies these effects when compared to material properties. In this study, gender difference is not discussed due to the limited sample size. However, the effect of gender is important for chest injury. Scenario 4 where morphomics data is added to the vehicle and demographic data, the effect of gender is important to predict rib fracture, which was not significantly important only by using vehicle and demographic variables (Scenario 2).

Prox. end inner angle and *Prox. end highest curvature* which tended to increase the rib fracture risk are age-related shape changes. Therefore, rib shape change is important factor when we consider the risk of rib fracture in real-world crashes.

In this study, the statistical model selected the parameterization of a rib's in-plane shape from morphomic variable and rib's out-of-plan factors such as pump-handle angle, lateral swing angle and bucket-handle angle[10] are not included. To avoid the problem of over-fitting caused by the extra terms corresponding to the size of the model, the model presented focuses only in-plane shape. In addition, the model did not include the effect of changes in material and thickness of cortical bone to predict the rib fracture due to the limited sample size. By increasing the number of crash cases, these analyses will have more statistical power to investigate the contribution of these factors compared to geometry.

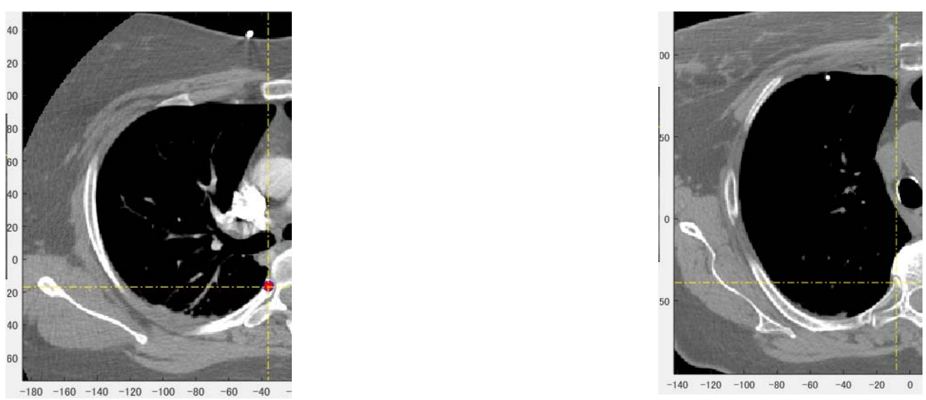

(a) 40 yr.
Prox. inn angle 100.5 deg
Prox. end highest curvature 4.6

(b) 82 yr.
Prox. inn angle 134.6 deg,
Prox. end highest curvature 10.3

Fig. 8. Sagittal plane image at start point of rib 5

V. CONCLUSIONS

This study used detailed injury and crash data in conjunction with medical imaging from the ICAM and morphomics databases to evaluate the effect of rib shape in frontal crashes. Results, confirmed with real-world crash cases, demonstrate that rib fracture patterns in older occupants were more anterior compared to younger occupants. Multivariate analysis with vehicle, demographic, and morphomics variables predicted the rib fracture risk and assessed the importance of individual predictors. Morphomics variables in this study showed that elderly rib shape is important when predicting rib fracture risk. This paper introduced a method to quantify elderly rib fractures using analytic morphomics in an accurate and systematic manner. The characterization of the elderly can then be used as a data source to provide relevant geometric data to inform tailored human finite element ribcage models.

VI. ACKNOWLEDGEMENT

The authors are grateful for the assistance of the Morphomic Analysis Group (MAG) image processing team in the University of Michigan.

VII. REFERENCES

[1] United Nations Department of Economic and Social Affairs "Percentage by Broad Age Groups" Internet: [http://esa.un.org/unpd/wpp/Download/Standard/Population/], The 2012 Revision.

[2] e-Stat. "Japanese police annual report on road traffic fatal accidents and traffic law enforcement violations" Internet: [http://www.e-stat.go.jp/SG1/estat/List.do?lid=000001142617]

[3] Mulligan GWN, Pizey G, Lane D, Andersson L, English C, and Kohut C, An introduction to the understanding of blunt chest trauma. In Biomechanics of Impact Injury and Injury Tolerances of the Thorax-Shoulder Complex, ed. Backaitis S, *Society of Automotive Engineers publication* PT-45, 1994, 11-36

[4] Kent R, Lee S-H et al., Structural and material changes in the aging thorax and their role in crash protection for older occupants, *Stapp Car Crash Journal,* 2005, Vol.49: 231-249.

[5] Antona-Makoshi J, Yamamoto Y et al., Age-dependent factors affecting thoracic response: a finite element study focused on Japanese elderly occupants. *Traffic Injury Prevention*, 2015, Vol.16: 66-74.

[6] Schoell S.L, Weaver A.A et al., Development and validation of an older occupant finite element model of a mid-size male for investigation of age-related injury risk. *Stapp Car Crash Journal,* 2015, Vol.59: 359-383.

[7] Shi X, Cao L, Reed M, Rupp J, and Hu J, Effect of obesity on occupant responses in frontal crashes: a simulation analysis using human body models, *Computer Methods in Biomechanics and Biomedical Engineering*, 2015, Vol. 18, No.12: 1280-1292.

[8] Iwamoto M, Nakahira Y, Kimpara H, and Min K, Development of a finite element model of 5th percentile female with multiple muscle and its application to investigation on impact response of elderly females, *Proceeding of the 23rd International Techinical Conference on the Enhanced Safety of Vehicle*, 2013, 13-0366

[9] Schoell S, Weaver A, Vavalle N, and Stitzel J, Age- and sex-specific thorax finite element model development and simulation, *Traffic Injury Prevention*, 2015, Vol.16: 57-65.

[10] Poulard D, Chen H, Crandall J, Dziewonski T, Pedzisz M, Panzer M, Component-level biofidelity assessment of morphed pedestrain finite element models. Proceeding of IRCOBI Conference, 2015, Lyon, France.

[11] Holcombe S, Kindig M, et al., Age-based predictive model of the pediatric ribcage, *International Journal of Automotive Engineering*, 2014 Vol. 5: 15-22.

[12] Holcombe S, Wang SC, Grotberg JB, Parametric modeling of human rib centroid geometry, *Journal of Biomechmaics* (in review process).

[13] Stitzel JD, Kilgo PD, et al., Age thresholds for increased mortality or predominant crash induced thoracic injuries. *Annals of Advances in Automotive Medicine* 2010, No.54: 41-50.

[14] Ritchie N, Schneider L, Wang SC, and Sochor M, A method for documenting location of rib fractures for occupants in real-world crashes using medical computed tomography (CT) scans, Warrendale, PA: SAE; 2006. *SAE Technical paper* 2006-01-0250.

[15] Zhang P, Parenteau C, et al. Prediction of thoracic injury severity in frontal impacts by selected anatomical morphomic variables through model-averaged logistic regression approach, *Accident Analysis and Prevention*, 2013, Vol.5: 172-180.

[16] Parenteau C, Zhang P, et al. Can anatomical morphomic variables help predict abdominal injury rates in frontal vehicle crashes, *Traffic Injury Prevention*, 2014, Vol.15: 619-626.

[17] Kindig M and Kent R, Characterization of centroid geometry of human ribs, *Journal of Biomechanical Engineering*, 2013, 135(11): 111007.

[18] Hanna R, Hershman L, Evaluation of thoracic injuries among older motor vehicle occupants, Washington, DC: NHTSA; 2009. DOT HS 811101.

[19] Lee E, Craig M, and Scarboro M, Real-world rib fracture patterns in frontal crashes in different restraint conditions, *Traffic Injury Prevention*, 2015, Vol.16: 115-123.

[20]Kemper A, McNally C, Pullins C, Freeman L, Duma S, and Rouhana S, The biomechanics of humans ribs: material and structural properties from dynamic tension and bending tests. *Stapp Car Crash Journal*, 2007, Vol51: 235-273.